Available online at www.sciencedirect.com

ScienceDirect

International Journal of Mass Spectrometry 255–256 (2006) 225–231

International Journal of Mass Spectrometry

www.elsevier.com/locate/ijms

Gas-phase ion chemistry of Si^+ and NF_3: An experimental and theoretical study

P. Antoniotti [*], L. Operti, R. Rabezzana [**], F. Turco, G.A. Vaglio

Dipartimento di Chimica Generale ed Organica Applicata and NIS Centre of Excellence, Università degli Studi di Torino,
Corso Massimo d'Azeglio 48, 10125 Turin, Italy

Received 30 November 2005; received in revised form 4 January 2006; accepted 5 January 2006
Available online 15 February 2006

Dedicated to Professor Diethard K. Böhme on the occasion of his 65th birthday.

Abstract

The study of the gas-phase reactions of the Si^+ ions with nitrogen trifluoride (NF_3) was performed by quadrupole ion trap mass spectrometry and ab initio calculations. Experimental results display a thermodynamically favoured reaction cascade starting from the reactants corresponding to multiple fluorine abstraction, which ultimately yields neutral fluorosilane by fluoride abstraction. A parallel, slightly endothermic channel is observed starting from the reactants and generating the $NF_2{}^+$ and SiF products. The study of the potential energy hypersurface of the $Si^+(^2P) + NF_3$ system evidenced the initial formation of the N-coordinated $Si^+–NF_3$ adduct. Subsequent rearrangements and atom migrations lead to the $FSi^+–NF_2$ isomer, whose dissociation yields SiF^+ and NF_2 as products. Theoretical energy profiles show that this pathway is strongly exothermic (about $-100\ kcal\ mol^{-1}$) and that the dissociation of the $FSi^+–NF_2$ species to the endothermic ($+6\ kcal\ mol^{-1}$) channel products ($NF_2{}^+$ and SiF) is extremely unlikely for ground-state reactants.

Keywords: Gas-phase ion chemistry; Ab initio calculations; Ion trap mass spectrometry; Silicon ions; Nitrogen trifluoride

1. Introduction

Nitrogen trifluoride, NF_3, is one of the most extensively used perfluorocompounds (PFCs) in the semiconductor industry to perform etching and cleaning processes by plasma techniques [1–6]. With respect to more traditional fluorinated gases, such as CF_4 and C_2F_6, NF_3 offers advantages of avoidance of carbon contamination residues and shorter lifetime. However, with its atmospheric lifetime of 740 years, NF_3 still represents a potential greenhouse gas. Therefore, it is important to find a method to quantitatively measure its concentration in the atmosphere. To this purpose, Li^+ ion attachment mass spectrometry was proposed as a technique to quantify the emissions of the PFCs [7]. In addition, in the past years several experimental and theoretical results have been obtained on the gas-phase reactions of NF_3. Studies on the Brönsted and Lewis basicities of NF_3 and on the reactivity of NF_3H^+ were performed, showing that NF_3 behaves as a bi-functional base in the gas phase, which can bind acid species at both nitrogen and fluorine [8–14]. Moreover, a computational study was performed on the reaction of NF_3 and O (^{1}D), as a conceivable source of FO radicals [15].

With the aim to extend the knowledge on the reactivity of NF_3 in the gas phase and to test the feasibility of NF_3 detection by ion attachment mass spectrometry, we performed the present study of the gas-phase reaction of Si^+ and NF_3, both by mass spectrometric and computational approaches. Moreover, the present results may help to unravel the ionic processes occurring during the deposition and etching of silicon-based surfaces starting from gaseous mixtures containing NF_3 and silane, which yields Si^+ ions in appreciable amounts when ionised.

2. Methods

2.1. Theoretical methods

The study of Si^+ with NF_3 was carried out by determining, on the relevant energy hypersurface, the critical points corre-

---

[*] Corresponding author. Tel.: +39 011 6707519; fax: +39 011 6707591.
[**] Corresponding author. Tel.: +39 011 6707587; fax: +39 011 2367587.
E-mail addresses: paola.antoniotti@unito.it (P. Antoniotti), roberto.rabezzana@unito.it (R. Rabezzana).

1387-3806/$ – see front matter © 2006 Elsevier B.V. All rights reserved.
doi:10.1016/j.ijms.2006.01.010

sponding to stable and transition structures (TS). The geometries of the species involved in the reaction have been first optimised by analytical-gradient techniques at the UMP2(full) (second order unrestricted Møller–Plesset perturbation theory including all electrons in the correlation calculation) level of theory [16,17]. The UMP2(full) geometries were characterized as energy minima or first order saddle points by diagonalization of the analytically computed Hessian (vibrational frequencies calculations) [18]. The intrinsic reaction coordinate (IRC) procedure [19,20] was applied, at the UMP2(full) level of theory, in order to unambiguously connect the transition structures to the relevant reactants and products. The standard basis set used herein was triple ζ plus polarization basis set labelled 6–311G(d) [21–25].

The UMP2(full)/6–311G(d) geometries were then used to recompute the relative energies at the Coupled Cluster level of theory, including the contribution from single and double substitution and an estimate of connected triples, CCSD(T,full) [26,27] (including all electrons in the correlation calculation) in conjunction with the 6–311G(d) basis set.

The quantum chemical calculations have been performed using the GAUSSIAN03 [28] system of programs, installed on Alphaserver xp1000 and HPworkstation xw8200.

2.2. Mass spectrometry experiments

Nitrogen trifluoride was supplied by Praxair (Oevel, Belgium) at 99.99% purity grade. Si^+ ions were generated by 35 eV electron ionisation of silane, purchased by SIAD (Bergamo, Italy) at 99.99% purity grade. Before using, each reagent gas was dried by sodium sulphate. Helium buffer gas was supplied by SIAD (Bergamo, Italy) at an extra-high purity grade and was used without further purification. All the experiments were run on a Finnigan (Austin, TX, USA) ITMS instrument maintained at 333 K. Pressures were measured by a Bayard Alpert ion gauge and corrected for both the relative sensitivity of the ion gauge with respect to different gases[1] [29] and a calibration factor, which depends on the geometry of the instrument, determined as reported previously [30]. Pressures were typically 6.0×10^{-7} Torr for each reagent gas and 3.0×10^{-4} Torr for helium (1 Torr = 133 Pa). At this buffer gas pressure, empirically set in order to maximize the abundance of the signals, it is reasonable to suppose that most of the reactant ions are kinetically thermalized. The scan modes for ion/molecule reaction experiments used to determine reaction sequences and rate constants for reaction of selected ions, and the corresponding calculation procedures have been previously described in detail [30]. Selective isolation of ions was achieved by the apex method (superimposition of dc and rf voltages). In all experiments ions were detected in the 10–300 Th range. Experiments for the determination of each rate constant were repeated two or three times and the results reported here are the means of the calculated values.

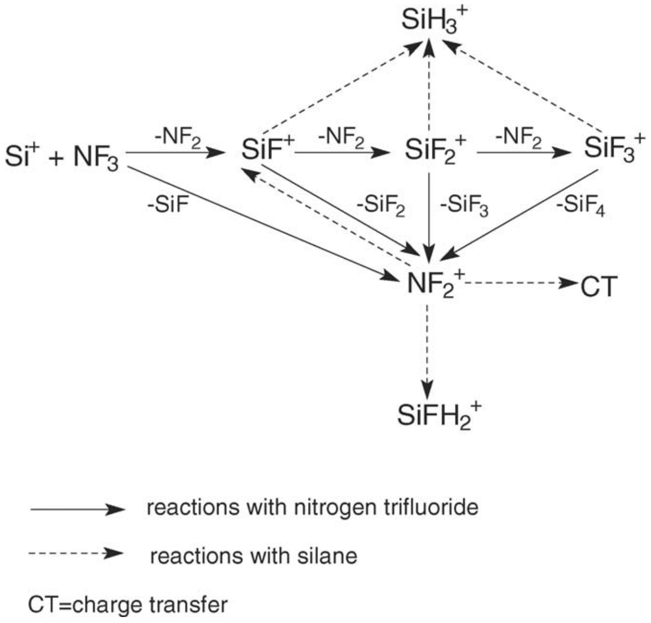

Scheme 1.

3. Results and discussion

3.1. Experimental results

Scheme 1 reports the reaction sequences starting from Si^+ and NF_3; the same reactions are listed in Table 1. As in our ion trap device the ionisation and reaction events occur in the same place, i.e., the ion trap itself, neutral silane, which yields the Si^+ ions by ionisation, is also present when the selected ions are stored and react with the neutrals in the trap. Therefore, reactions with silane occur too, and reactions of ions formed starting from Si^+ and NF_3 with SiH_4 are also reported in the Table for comparison. For all the reactions reported, experimental and collisional rate constants, reaction efficiencies and reaction enthalpies, when thermochemical data were available, are listed in the Table. The reaction cascade starting from Si^+ and NF_3 displays two distinct features, corresponding to fluorine and fluoride abstraction. In the first case, the reaction sequence proceeds up to formation of the SiF_3^+ ion, where there are no more electrons available for covalent bonds on the Si atom; in fact, SiF_3^+ only undergoes fluoride abstraction in the reaction with NF_3, yielding the thermochemically favoured neutral SiF_4. Fluoride abstraction also occurs as a parallel channel in the reactions of the SiF_n^+ ($n = 0$–2) ions, yielding the same ion product, NF_2^+, and different neutral silicon fluorides. This kind of reaction becomes thermodynamically more favoured with increasing number of F atoms in the reactant ion and hence in the neutral yielded. In fact, the heats of formation of the neutrals formed become more negative and those of the reactant ions less positive with increasing number of F atoms. It is worth noting that for the SiF_n^+ ($n = 0, 1$) ions these reactions are slightly endothermic; nonetheless, they are clearly observed, even if with low rate constants. These endothermic channels are likely ascribed to the presence of excited reactant ions; thermalization was therefore attempted by introducing a cooling time before ion isolation (up to 40 ms), by decreasing

---

[1] M. Decouzon, J.-F. Gal, P.-C. Maria, A.S. Tchinianga, personal communication.

Table 1
Ion/molecule reactions in the Si^+/NF_3 system[a]

	Reaction	k_{exp}	Σk_{exp}	k_{cap}[b]	efficiency[c]	ΔH[d]
(1)	$Si^+ + NF_3 \rightarrow SiF^+ + NF_2$	3.4				−93.4
(2)	$\rightarrow NF_2{}^+ + SiF$	1.2	4.6	10.47	0.44	+6.9
(3)	$SiF^+ + NF_3 \rightarrow SiF_2{}^+ + NF_2$	1.3				−16.5
(4)	$\rightarrow NF_2{}^+ + SiF_2$	0.21	1.5	8.830	0.17	+3.1
(5)	$SiF^+ + SiH_4 \rightarrow SiH_3{}^+ + SiFH$	0.42	0.42	11.15	0.038	
(6)	$SiF_2{}^+ + NF_3 \rightarrow SiF_3{}^+ + NF_2$	1.5				−92.2
(7)	$\rightarrow NF_2{}^+ + SiF_3$	4.3	5.8	8.030	0.72	−39.4
(8)	$SiF_2{}^+ + SiH_4 \rightarrow SiH_3{}^+ + SiF_2H$	9.4	9.4	10.48	0.90	
(9)	$SiF_3{}^+ + NF_3 \rightarrow NF_2{}^+ + SiF_4$	6.0	6.0	7.551	0.79	−55.2
(10)	$SiF_3{}^+ + SiH_4 \rightarrow SiH_3{}^+ + SiF_3H$	8.8	8.8	10.09	0.87	
(11)	$SiH_3{}^+ + NF_3 \rightarrow NFH^+ + SiF_2H_2$	0.22				
(12)	$\rightarrow SiF^+ + [N, F_2, H_3]$	0.40				
(13)	$\rightarrow SiFH^+ + [N, F_2, H_2]$	0.26				
(14)	$\rightarrow SiFH_2{}^+ + [N, F_2, H]$	1.2				
(15)	$\rightarrow NF_2{}^+ + SiFH_3$	1.9				
(16)	$\rightarrow SiF_2H^+ + [N, F, H_2]$	0.58	4.6	10.10	0.45	
(17)	$NF_2{}^+ + SiH_4 \rightarrow$ charge transfer	1.7				−14.5
(18)	$\rightarrow SiF^+ + [N, F, H_4]$	0.27				−196.9[e]
(19)	$\rightarrow SiFH_2{}^+ + [N, F, H_2]$	0.77	2.7	10.94	0.25	

[a] Rate constants are expressed as 10^{-10} cm^3 molecule^{-1} s^{-1}; uncertainty is within 20%.

[b] Collisional rate constants were calculated according to the Parameterized Trajectory Theory [31] taking the polarizabilities of nitrogen trifluoride and of silane and the dipole moment of nitrogen trifluoride from ref [32].

[c] Efficiency was calculated as the ratio $\Sigma k_{exp}/k_{cap}$.

[d] Standard reaction enthalpies (kcal mol^{-1}) calculated from experimental data taken from ref [33].

[e] Reaction enthalpy calculated by assuming the formation of the HF and NH_3 neutral molecules.

the q_z value at which the reactant ion was stored (q_z lowest value = 0.3), and by using a buffer gas mixture of He and Ar (in the ratio of about 1:1, total pressure = 3.0×10^{-4} Torr). Despite all these attempts, the endothermic products were still detected, even with a formation rate constant reduced of about 20%. The thermalization procedures employed allowed to observe also the effect of the variation of the ion kinetic energy on the exothermic reactions. In particular, the Si^+ ions yield exothermic products with both NF_3 (SiF^+, reaction (1), Table 1), and SiH_4 ($Si_2H_2{}^+$). This latter reaction, together with all the self-condensation ion/molecule reactions occurring in silane, were previously studied [30] and therefore are not reported in the Table. The experiments performed show an increase of the rate constants with decreasing ion kinetic energy, especially with decreasing q_z value. For the reaction:

$$Si^+ + SiH_4 \rightarrow Si_2H_2{}^+ + H_2 \qquad (1)$$

the experimental k value increases from 4.2×10^{-10} cm^3 molecule^{-1} s^{-1} at $q_z = 0.8$ to 5.8×10^{-10} cm^3 molecule^{-1} s^{-1} at $q_z = 0.32$. Reactions of Si^+ reported in Table 1 were performed at $q_z = 0.45$, a q_z value which allows to obtain both good trapping and thermalization efficiencies of the ions, where the rate constant of reaction (1) resulted to be 5.7×10^{-10} cm^3 molecule^{-1} s^{-1}. This value is in appreciable agreement with that obtained by FTICR experiments by using deuterated silane, 6.9×10^{-10} cm^3 molecule^{-1} s^{-1} [34]. Therefore, we are confident that the experimental rate constants reported do not considerably differ (at least within 20%) from those obtained by more acknowledged methods such FTICR and that, for this reason, they could be safely considered as reliable kinetic data. As far as the occurrence of the endothermic reactions is concerned, incomplete quenching of the ion kinetic energy and/or the presence of a fraction of electronically excited ions must be assumed (for Si^+, the first excited state, ^4P, lies 5.3 eV above the ^2P ground state [35]).

Formation of neutral silicon fluorides is a common pathway also in the reactions of $SiF_n{}^+$ (n = 1–3) with silane; all these reactions lead to the same ionic product, $SiH_3{}^+$, through hydride abstraction, thus generating the corresponding neutrals SiF_nH (n = 1–3). Hydride abstraction is always faster than fluoride abstraction, probably because is less sterically hindered. For the $SiF_2{}^+$ and $SiF_3{}^+$ ions, both H^- and F^- abstractions are very fast; to the contrary, for low-valence Si-ions (Si^+ and SiF^+) formation of covalent bonds is favoured with respect to anion abstraction: in particular, Si^+ does not undergo hydride abstraction, as it reacts with silane to yield the $Si_2H_2{}^+$ ion product [30].

The $NF_2{}^+$ ion is unreactive towards NF_3 under the experimental conditions used here, but reacts with silane mainly by charge transfer. Minor reaction channels correspond to formation of SiF^+ and $SiFH_2{}^+$. Although their formation implies a considerable number of rearrangements, it is probable that the high Si–F bond energy [32] constitutes an effective driving force for these reactions. The formation of ionic instead than neutral fluorosilanes is ascribed to the lower ionization energy of the $SiFH_n$ (n = 0, 2) neutrals compared to those of NH_3 + HF and monofluoroamine, respectively, these latter being the neutrals likely formed in these reactions [33]. The ionization energy of $SiFH_2$ is not available in the literature, but is expected to be lower than that of NFH_2, on the basis of the experimental results.

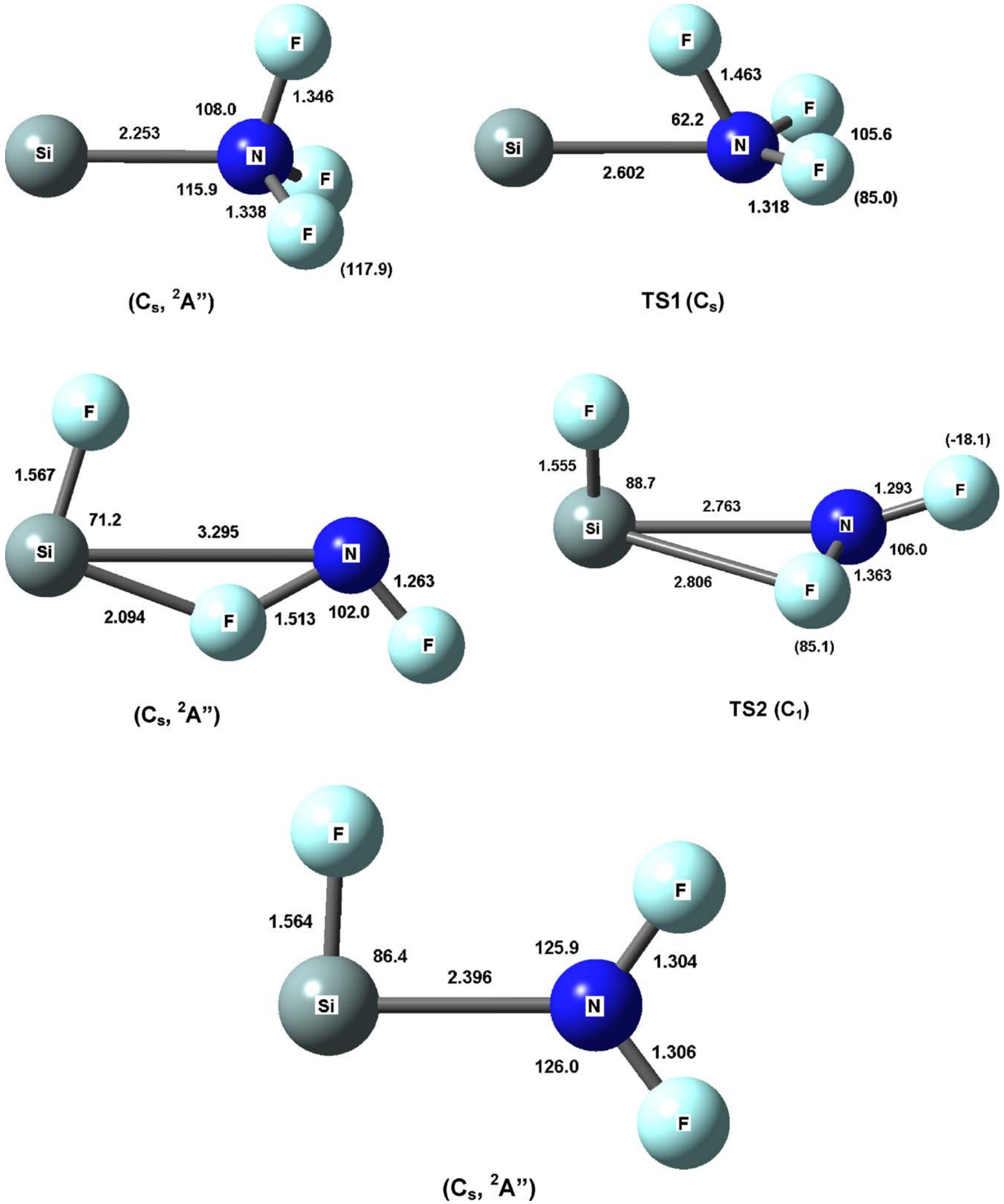

Fig. 1. Geometrical parameters of the Si–NF$_3^+$, FSi–F–NF$^+$, and FSi–NF$_2^+$ minima and of their interconnecting transition structures TS1 and TS2. Bond distances are in Ångström, and bond angles in degrees; dihedral angles (in parentheses) are defined as FSiNF, where the reference F lies on the sheet plane.

3.2. *Theoretical results*

In this work we report the preliminary theoretical results of the reactions of Si$^+$ and NF$_3$ observed in the mass spectrometric experiments:

$$\mathrm{Si}^+ + \mathrm{NF}_3 \rightarrow \mathrm{SiF}^+ + \mathrm{NF}_2 \qquad (2)$$

$$\rightarrow \mathrm{NF_2}^+ + \mathrm{SiF} \qquad (3)$$

Table 2
Total, relative energies and enthalpies (hartree and kcal mol^{-1}) for the reaction Si$^+$ (^{2}P) + NF$_3$

Species	UMP2(full)[a]	ΔE	H^{298}[b]	ΔH^{298}	CCSD(T,full)[c]	ΔE	$\Delta H^{298}_{\mathrm{exp}}$[d]
Si$^+$ (^{2}P) + NF$_3$	−642.231972	0.0	−642.214495	0.0	−642.281212	0.0	
Si–NF$_3{}^+$ (^{2}A″)	−642.255273	−14.6	−642.236661	−13.9	−642.303051	−13.7	
TS1	−642.247520	−9.8	−642.230502	−10.0	−642.295923	−9.2	
FSi–F–NF$_2{}^+$ (^{2}A″)	−642.397999	−104.2	−642.380972	−104.5	−642.446080	−103.5	
TS2	−642.388254	−98.1	−642.371572	−98.6	−642.436408	−97.4	
FSi–NF$_2{}^+$ (^{2}A″)	−642.395220	−102.4	−642.377112	−102.0	−642.443277	−101.7	
SiF$^+$ ($^1\Sigma^+$) + NF$_2$ (^{2}B$_1$)	−642.379945	−92.8	−642.363949	−93.8	−642.428460	−92.4	−93.4
SiF ($^2\Pi$) + NF$_2{}^+$ (^{1}A$_1$)	−642.222756	+5.8	−642.205475	+5.7	−642.271490	+6.1	+6.9

[a] Calculated using a basis set 6–311G(d).

[b] The energies calculated at the UMP2(full) are combined with the thermal energy correction to the enthalpy predicted by frequencies calculations.

[c] Calculated using a basis set 6–311G(d) and UMP2/6–311G(d) optimized geometries.

[d] Calculated from experimental formation enthalpies [33].

In ab initio theoretical calculations the following chemical processes were considered: (1) the formation of the initial Si–NF$_3{}^+$ adduct from Si$^+$ and NF$_3$; (2) the rearrangement of a fluorine atom, giving FSi–F–NF$^+$ species; (3) the isomerization of FSi–F–NF$^+$ into FSi–NF$_2{}^+$species; (4) the dissociation of FSi–NF$_2{}^+$ in the fragment SiF$^+$ and NF$_2$ or SiF and NF$_2{}^+$.

The geometrical parameters of the three intermediates and of their interconnecting transition structures (TS1 and TS2) are shown in Fig. 1. The total and relative energies at the UMP2(full)/6–311G(d) and CCSD(T,full)/6–311G(d) level of theories are listed in Table 2. In this Table are also reported the total and relative enthalpies calculated combining the UMP2(full) energies with the thermal correction to the enthalpy predicted by frequencies calculations. Fig. 2 shows a diagrammatic energy profile at the CCSD(T,full)/6–311G(d) level of calculation.

A preliminary step of this study has been to investigate the behaviour of NF$_3$ as bi-functional Lewis base when interacting with Si$^+$. Recent experimental and theoretical studies on the ligation of NF$_3$ to ionic Lewis acids as H$^+$, Li$^+$, CH$_3{}^+$ and NF$_2{}^+$ indicate that both isomeric structures, with the ion bound to the N and the F atom of NF$_3$, can exist in gas phase and that the nature of the electrophile has an important effect on the relative stability of the two isomers [8,36].

The results of our calculations on the interaction between Si$^+$ (^{2}P) with NF$_3$ have pointed out that only the adduct Si–NF$_3{}^+$ exists. The adduct arising from coordination of Si$^+$ (^{2}P) to the fluorine atom(s) of NF$_3$, despite careful searching, has not been located.

The initial adduct Si–NF$_3{}^+$ (^{2}A″), with C$_s$ symmetry, lies 13.7 kcal mol^{-1} below the reagents Si$^+$ (^{2}P) and NF$_3$, at the CCSD(T,full) level of theory. The Si–N bond, 2.253 Å, is longer than the same bond in Si–NH$_2{}^+$, 1.663 Å, where the amino group acts as an extremely strong π-donor generating an Si–N multiple bond [37] but is shorter than the Si–N distance in the SiH$_4$·NH$_3$ adduct, 3.2–3.4 Å, where no donor–acceptor bond is formed between the molecules [38].

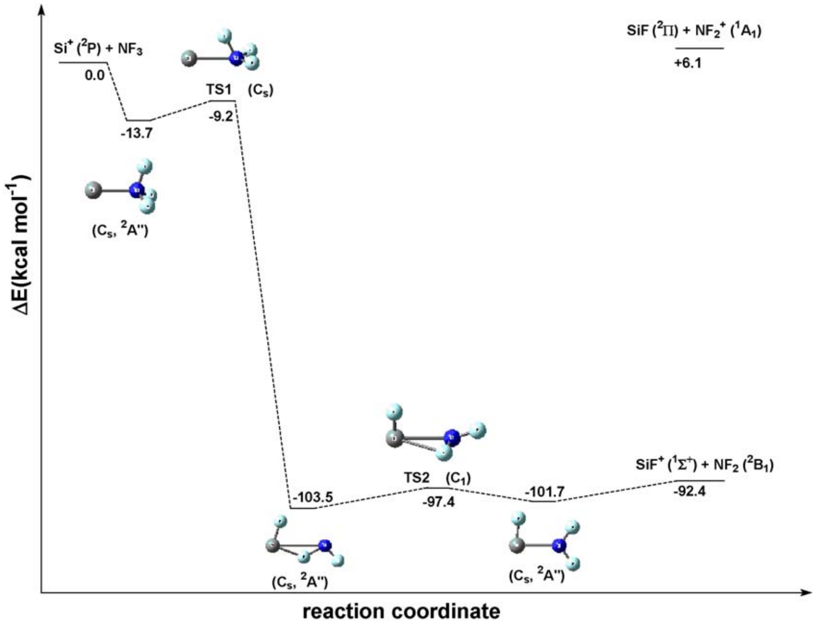

Fig. 2. Relative energies (kcal mol^{-1}), calculated at the CCSD(T,full)/6–311G(d) level of theory, of the species involved in the reaction between Si$^+$(^{2}P) and NF$_3$.

The second step of the reaction is the rearrangement of Si–NF_3^+ into the FSi–F–NF^+ ($^2A''$) isomer, whose geometrical parameters are shown in Fig. 1. This minimum, with a C_s symmetry, is the most stable species on the surface lying 89.8 kcal mol^{-1} below the adduct Si–NF_3^+ at the CCSD(T,full) level of theory. In this isomer the lengthening of the Si–N distance up to 3.3 Å, which is only slightly smaller than the sum of the van der Waals radii of silicon (2.00 Å) and nitrogen (1.54 Å) [38], points to a weak interaction between Si and N atoms not leading to formation of the Si–N chemical bond. The donor–acceptor interaction is between the silicon atom and a fluorine atom bound to nitrogen. The distances of the fluorine atom bridged between silicon and nitrogen are, respectively, 2.094 Å and 1.513 Å, which are quite longer than the usual bond distance Si–F and N–F.

The rearrangement of Si–NF_3^+ into the FSi–F–NF^+ isomeric structure occurs through the transition structure TS1 (C_s), whose single imaginary frequency of −124.8 cm^{-1} refers to the concerted motion of the fluorine atom and the NF_2 fragment. This isomerization takes place by cleavage of the F–N bond and followed by reassociation through formation of a Si–F bond, at the same time the NF_2 fragment migrates from fluorine to silicon. As evidenced by Fig. 1, the Si–N, 2.602 Å, and N–F, 1.463 Å, TS1 bond distances are significantly elongated with respect to the Si–N, 2.253 Å, and N–F, 1.345 Å, distances of the adduct. Moreover, the SiNF bond angle, 62.2°, results quite close to the same angle of the adduct. Despite the significant structural reorganization required to pass from Si–NF_3^+ to FSi–F–NF^+ the TS1 geometry is more similar to the adduct and reflects also in the activation barrier of only 4.5 kcal mol^{-1}.

The third step of the reaction consists of the further rearrangement of the geometrical parameters from FSi–F–NF^+ into the FSi–NF_2^+ isomer. The FSi–NF_2^+ ($^2A''$) ion has a planar geometry (C_s) and lies only 1.8 kcal mol^{-1} above the FSi–F–NF^+ species, at the CCSD(T,full) level of theory. The Si–N bond distance, 2.396 Å, is longer than the same bond in the adduct, 2.253 Å; despite the planar structure, the bond length is typical of single donor–acceptor interaction.

The geometry of the transition structure TS2 (C_1), that interconnects the two minima FSi–F–NF^+ and FSi–NF_2^+, is presented in Fig. 1; the single imaginary frequency of 101.0 cm^{-1} refers to the rotation of the NF_2 fragment. This motion is accompanied by cleavage of the Si–F bond and followed by formation of the Si–N bond. This is also exemplified by the bond distance in the TS2: the Si–F bond, 2.806 Å, is significantly elongated and the Si–N bond, 2.763 Å, is shortened with respect to the corresponding parameters of the FSi–F–NF^+ species. This transition structure is associated to an energy barrier of only 6.1 kcal mol^{-1} at the CCSD(T;full) level of theory.

The last step of the reaction is the etherolytic Si–N bond cleavage of the FSi–NF_2^+ intermediate and the ensuing formation of the SiF^+ ($^1\Sigma^+$) and NF_2 ($^2B_1$) products. This process takes place without formation of a transition structure (the reverse process has no barrier to overcome). The energy difference between FSi–NF_2^+ and the products is only 9.3 kcal mol^{-1} at the CCSD(T,full) level of calculation.

The overall reaction from reagents, Si^+ (^2P) and NF_3, to the products, SiF^+ ($^1\Sigma^+$) and NF_2 ($^2B_1$), is exoergic by 92.4 kcal mol^{-1}, at the CCSD(T,full) level of theory. The reaction enthalpy of −93.8 kcal mol^{-1}, calculated at the UMP2(full) level of theory, including the thermal correction to enthalpy determined in the frequencies calculations, is in good agreement with the experimental reaction enthalpy of −93.4 kcal mol^{-1} (Table 1) [33].

Mass spectrometric experiments also display a parallel pathway resulting in the formation of the NF_2^+ ($^1A_1$) and SiF ($^2\Pi$) products (reaction (2), Table 1). This process is slightly endoergic by 6.1 kcal mol^{-1} at the CCSD(T,full) level of the theory. Also in this case the reaction enthalpy of 5.7 kcal mol^{-1}, calculated at the UMP2(full) level of theory, is in agreement with the experimental reaction enthalpy of 6.9 kcal mol^{-1}, determined from the reagents and the products standard formation enthalpy [33].

4. Conclusions

The theoretical investigation of the potential energy hypersurface of the gas-phase reactions of Si^+(^2P) and NF_3 indicates that the initial ion/neutral adduct is formed via coordination of the lone pair of the nitrogen atom to the reactant ion. Subsequently, the adduct rearranges to the most stable minimum on the hypersurface with FSi–F–NF^+ connection, where a F atom is migrated to the Si atom coordinated to the NF_2 moiety through a F lone pair. This minimum further rearranges to the N-coordinated FSi–NF_2^+ adduct, which lies slightly higher in energy (about +2 kcal mol^{-1}). Heterolytic Si–N bond cleavage starting from this adduct leads to the SiF^+ and NF_2 exothermic reaction products, and takes place with no energy barrier in excess with respect to the products enthalpies. Experimental data display a reaction sequence consisting of multiple exothermic F-atom abstractions, in agreement with the theoretical investigation of the first reaction step. However, a parallel channel is also observed in ITMS experiments, leading to the NF_2^+ and SiF products, which is weakly endothermic. The occurrence of this reaction indicates the incomplete ion thermalization, which could not be avoided despite our efforts. Experimental data regarding successive reaction steps with both NF_3 and SiH_4 neutrals seem to indicate the formation of neutral fluorosilanes as favorite products. Therefore, future work will deal with the experimental investigation of the complete SiH_4/NF_3 system in order to find further evidence of the paths detected in the present work, and with the theoretical study of the most interesting features evidenced by experimental results.

Acknowledgements

The authors would like to acknowledge financial supports from the University of Turin and from the Italian MIUR through the ‘Cofinanziamento di Programmi di Ricerca di Rilevante Interesse Nazionale’.

References

[1] F. Ishii, Y. Kita, Advanced Inorganic Fluorides, Elsevier, Amsterdam, 2000.
[2] Yu.V. Fominski, O.I. Naoumenko, V.N. Nevolin, A.P. Alekhin, A.M. Markeev, L.A. Vyukov, Appl. Phys. Lett. 68 (1996) 2243.
[3] J.B. Casady, E.D. Luckovski, M. Bozack, D. Sherida, R.W. Johnson, J.R. Williams, J. Electrochem. Soc. 143 (1996) 1750.
[4] E. Meeks, R.S. Larson, S.R. Vosen, J.W. Shon, J. Electrochem. Soc. 144 (1997) 357.
[5] J.G. Langan, S.W. Rynders, B.S. Felker, S.E. Beck, J. Vac. Sci. Technol. A 16 (1998) 2108.
[6] B.E.E. Kastenmeier, G.S. Oehrlein, J.G. Langan, W.R. Entley, J. Vac. Sci. Technol. A 18 (2000) 2102.
[7] S. Arulmozhiraja, T. Fujii, J. Phys. Chem. A 104 (2000) 9613.
[8] F. Grandinetti, J. Hrušàk, D. Schöder, S. Karrass, H. Schwarz, J. Am. Chem. Soc. 114 (1992) 2806.
[9] F. Grandinetti, F. Pepi, A. Ricci, Chem. Eur. J. 2 (1996) 495.
[10] J.J. Fisher, T.B. McMahon, J. Am. Chem. Soc. 110 (1988) 7599.
[11] K. Hiraoka, M. Nasu, S. Fujimaki, S. Yamabe, J. Phys. Chem. 99 (1995) 822.
[12] F. Grandinetti, V. Vinciguerra, J. Mol. Struct. (Theochem.) 574 (2001) 185.
[13] P. Antoniotti, S. Borocci, F. Grandinetti, Eur. J. Inorg. Chem. 2004 (2004) 1125.
[14] K. Pei, J. Liang, H. Li, J. Mol. Struct. (Theochem.) 690 (2004) 159.
[15] P. Antoniotti, F. Grandinetti, Chem. Phys. Lett. 366 (2002) 676.
[16] C. Møller, M.S. Plesset, Phys. Rev. 46 (1934) 618.
[17] J.S. Binkley, J.A. Pople, Int. J. Quantum. Chem. 9 (1975) 229.
[18] J. Pople, A.P. Scott, M.W. Wong, L. Radom, Isr. J. Chem. 33 (1993) 345.
[19] C. Gonzales, H.B. Schlegel, J. Chem. Phys. 90 (1989) 2154.
[20] C. Gonzales, H.B. Schlegel, J. Phys. Chem. 94 (1990) 5523.
[21] R. Ditchfield, W.J. Hehre, J.A. Pople, J. Chem. Phys. 56 (1972) 2252.
[22] P.C. Hariharan, J.A. Pople, Theor. Chim. Acta 28 (1973) 213.
[23] M.M. Francl, W.J. Pietro, W.J. Here, J.S. Binkley, M.S. Gordon, D.J. Defrees, J.A. Pople, J. Chem. Phys. 77 (1982) 3654.
[24] K. Raghavachari, J.S. Binkley, R. Seeger, J.A. Pople, J. Chem. Phys. 72 (1980) 650.
[25] A.D. McLean, G.S. Chandler, J. Chem. Phys. 72 (1980) 5639.
[26] K. Raghavachari, G.W. Trucks, J.A. Pople, M. Head-Gordon, Chem. Phys. Lett. 157 (1989) 479.
[27] C. Hampel, K. Peterson, H.-J. Werner, Chem. Phys. Lett. 190 (1992) 1.
[28] M.J. Frisch, G.W. Trucks, H.B. Schlegel, G.E. Scuseria, M.A. Robb, J.R. Cheeseman, J.A. Montgomery Jr., T. Vreven, K.N. Kudin, J.C. Burant, J.M. Millam, S.S. Iyengar, J. Tomasi, V. Barone, B. Mennucci, M. Cossi, G. Scalmani, N. Rega, G.A. Petersson, H. Nakatsuji, M. Hada, M. Ehara, K. Toyota, R. Fukuda, J. Hasegawa, M. Ishida, T. Nakajima, Y. Honda, O. Kitao, H. Nakai, M. Klene, X. Li, J.E. Knox, H.P. Hratchian, J.B. Cross, C. Adamo, J. Jaramillo, R. Gomperts, R.E. Stratmann, O. Yazyev, A.J. Austin, R. Cammi, C. Pomelli, J.W. Ochterski, P.Y. Ayala, K. Morokuma, G.A. Voth, P. Salvador, J.J. Dannenberg, V.G. Zakrzewski, S. Dapprich, A.D. Daniels, M.C. Strain, O. Farkas, D.K. Malick, A.D. Rabuck, K. Raghavachari, J.B. Foresman, J.V. Ortiz, Q. Cui, A.G. Baboul, S. Clifford, J. Cioslowski, B.B. Stefanov, G. Liu, A. Liashenko, P. Piskorz, I. Komaromi, R.L. Martin, D.J. Fox, T. Keith, M.A. Al-Laham, C.Y. Peng, A. Nanayakkara, M. Challacombe, P.M.W. Gill, B. Johnson, W. Chen, M.W. Wong, C. Gonzalez, J.A. Pople, Gaussian 03, Revision B.05, Gaussian Inc., Pittsburgh PA, 2003.
[29] J.E. Bartmess, R.M. Georgiadis, Vacuum 33 (1983) 153.
[30] L. Operti, M. Splendore, G.A. Vaglio, A.M. Franklin, J.F.J. Todd, Int. J. Mass Spectrom. Ion Processes 136 (1994) 25.
[31] T. Su, W.J. Chesnavich, J. Chem. Phys. 76 (1982) 5183.
[32] R.D. Lide (Ed.), CRC Handbook of Chemistry and Physics, 73rd ed., CRC Press, Boca Raton, FL, 1992.
[33] P.J. Linstrom, W.G. Mallard (Eds.), Thermochemical data are taken from NIST Chemistry Webbook, NIST Standard Reference Database Number 69, National Institute of Standard and Technology, Gaithersburg MD, 20899, March 2003, http://webbook.nist.gov.
[34] M.L. Mandich, W.D. Reents Jr., M.F. Jarrold, J. Chem. Phys. 88 (1988) 1703.
[35] W.C. Martin, R. Zalubas, J. Phys. Chem. Ref. Data 12 (1983) 323.
[36] J.J. Fisher, T.B. McMahon, J. Am. Chem. Soc. 110 (1988) 7599.
[37] N. Goldberg, J. Hrušàk, M. Iraqi, H. Schwarz, J. Phys. Chem. 97 (1993) 10687.
[38] A.Y. Timoshkin, T.N. Sevast'yanova, E.I. Davydova, A.V. Suvorov, H.H. Schaefer, Russ. J. Gen. Chem. 72 (2002) 1576.